APPLICATION OF TURBULENCE MODELS TO NATURAL CONVECTION FROM A VERTICAL ISOTHERMAL PLATE

by

A. Heiss, J. Straub*, and I. Catton
Mechanical, Aerospace & Nuclear Engineering
University of California, Los Angeles, CA 90024-1597

*Lehrstuhl A fuer Thermodynamik
Technische Universitaet Munich, D-8000 Munich 2

"1988 National Heat Transfer Conference" in Houston USA

ABSTRACT

Several turbulence models have been tested for predicting low Reynolds number free convection boundary-layer flows on a vertical, heated surface. In the present study, only turbulence models were considered that can be used to calculate buoyancy driven wall boundary-layers without an a priori assumption with regard to profiles of velocity, temperature and the eddy diffusivity. Eight turbulence models are studied in the framework of stationary, two dimensional, Reynolds averaged boundary-layer equations of continuity, momentum and energy. These equations include the turbulent shear stress and heat transfer which are predicted by eddy-diffusion formulations (three mixing-length, k-ϵ and k-ϵ-$\overline{T'^2}$ model) and stress models (Reynolds stress model, algebraic and "corrected" algebraic stress model). The numerical results are compared with recently reported experimental data. All the models predict the heat transfer and mean flow characteristic reasonably well. The simplest models, however, using the mixing-length hypothesis, are not able to predict the transition from laminar to turbulent flow, whereas models based on solving transport equations for turbulent quantities calculate the transition ranges very well. This study shows that the low Reynolds number k-ϵ model by Lam and Bremhorst is the best tool to calculate turbulent vertical convective flows considering the quality of the results and the computer cost.

1. INTRODUCTION

The accurate modeling of turbulent free convection from a heated, flat plate is considered to be a logical first step towards the numerical simulation of more complex buoyancy affected turbulent flows. The parabolic forms of the differential equations allow a comparison between the quantities predicted by several turbulence models without high computer cost. It was not the aim of this study to develop a new turbulence model special for natural convection flow. This study shall show how well turbulence models optimized for turbulent flow without heat transfer or forced convection flow predict a rather uncomplicated natural convection flow without tuning the model constants, wall function or closure hypothesis.

Cheesewright and Ierokiopitis (1982) and Miyamato et al. (1982) have recently measured temperature and velocity simultaneously at essentially the same point in the flow. Using LDV techniques and very small thermocouples allowed them to obtain turbulent stress and heat flux distributions in addition to mean flow quantities. With this data, the numerical results can be compared with experimental data. The successful computation of Plumb and Kennedy (1977) and To and Humphrey (1986) encouraged this study.

2. NUMERICAL PROCEDURE

2.1 Mean Transport Equations

The starting point for the turbulence modeling effort in this study are the stationary, two-dimensional, Reynolds averaged boundary-layer equations of continuity, momentum and energy. The Boussinesq-approximation is used because the available experimental data are obtained in air with low overheat ratios $\frac{\Delta T}{T_o} \leq 0.2$. The conservation equations are

$$\frac{\partial \bar{u}}{\partial x} + \frac{\partial \bar{v}}{\partial y} = 0 \tag{1}$$

$$\frac{\partial(\bar{u}\bar{u})}{\partial x} + \frac{\partial(\bar{v}\bar{u})}{\partial y} = \frac{\partial}{\partial y}\left(\nu \frac{\partial \bar{u}}{\partial y} - \overline{u'v'}\right) + g\beta\left(\bar{T} - T_o\right) \tag{2}$$

$$\frac{\partial(\bar{u}\bar{T})}{\partial x} + \frac{\partial(\bar{v}\bar{T})}{\partial y} = \frac{\partial}{\partial y}\left(\alpha \frac{\partial \bar{T}}{\partial y} - \overline{v'T'}\right) \tag{3}$$

This system of differential equations for the mean flow quantities ($\bar{u}$, $\bar{v}$, $\bar{T}$) includes the turbulent shear stress $\overline{u'v'}$ and heat transfer $\overline{v'T'}$ which must be predicted by suitable closure hypotheses resulting from the turbulence models.

2.2. Turbulence Models

Table 1 shows the five tested turbulence models. The first three models follow the eddy-viscosity formulation, whereas with the last two models all turbulent second moments are calculated.

Table 1: Numbers of differential and algebraic equations.

Model	Differential eq.	Algebraic eq.
mixing-length model	$\bar{u}$, $\bar{T}$	ν_t
k-ε model	$\bar{u}$, $\bar{T}$, k, ε	ν_t
k-ε-$\overline{T'^2}$ model	$\bar{u}$, $\bar{T}$, k, ε, $\overline{T'^2}$	ν_t
Algebraic stress model	$\bar{u}$, $\bar{T}$, k, ε	$\overline{u'u'}$, $\overline{v'v'}$, $\overline{u'v'}$, $\overline{u'T'}$, $\overline{v'T'}$, $\overline{T'^2}$
Reynolds stress model	$\bar{u}$, $\bar{T}$, $\overline{u'u'}$, $\overline{v'v'}$, $\overline{w'w'}$, $\overline{u'v'}$, $\overline{u'T'}$, $\overline{v'T'}$, $\overline{T'^2}$, ε	

2.2.1. Eddy-Viscosity Formulation

Maintaining an analogy with laminar flow, the turbulent fluxes $\overline{u'v'}$ and $\overline{v'T'}$ are assumed to obey gradient type relations as follows,

$$-\overline{u'v'} = \nu_t \frac{\partial \bar{u}}{\partial y}$$

$$-\overline{v'T'} = \alpha_t \frac{\partial \bar{T}}{\partial y} \quad \text{with } Pr_t = \frac{\nu_t}{\alpha_t} \tag{4}$$

The turbulent viscosity ν_t is assumed to be proportional to a velocity scale and a length scale. A very simple way to obtain the turbulent viscosity is the mixing-length hypothesis. In this study three different mixing-length models (MMA, MMB, MMC) are compared without solving differential equations at a fixed turbulent Prandtl number $Pr_t = 0.9$,

Version A:
(Noto and Matsumoto, 1975)

$$\nu_t = 0.4\nu y^+[1 - \exp(-0.0017(y^+)^2)] \; ;$$

$$\text{with} \quad y^+ = \frac{y}{\nu}\left(\frac{\tau_w}{Q}\right)^{1/2}, \quad \text{and } \tau_w = \nu \left.\frac{\partial \bar{u}}{\partial y}\right|_{y=0} \tag{5}$$

Version B:
(Escudier, 1966)

$$\nu_t = (0.41y)^2 \left|\frac{\partial \bar{u}}{\partial y}\right| \quad \text{for } y/\delta \leq 0.22$$

$$\nu_t = (0.09\delta)^2 \left|\frac{\partial \bar{u}}{\partial y}\right| \quad \text{for } y/\delta > 0.22; \tag{6}$$

δ: boundary thickness

Version C:
(Cebeci and Khattab, 1975)

$$\nu_{ta} = [0.4y(1 - \exp(-y/A))]^2 \left|\frac{\partial \bar{u}}{\partial y}\right| \; ; \quad A = 26\,\nu\left(\frac{Q}{\tau_w}\right)^{1/2}$$

$$\nu_{tb} = [0.075\delta]^2 \left|\frac{\partial \bar{u}}{\partial y}\right| \tag{7}$$

$$\nu_t = \min(\nu_{ta};\nu_{tb})$$

The standard models try to bridge the gap between the full turbulent region and the wall using wall-laws for the mean flow quantities. This treatment doesn't allow transition calculations from laminar to turbulent flow nor does it yield good heat transfer results. In the present study, only low-Reynolds number turbulence models were considered, that can be used to calculate boundary layers without an a priori assumption with regard to profiles of velocity and temperature.

A more sophisticated way to determine the turbulent viscosity is to use k-ε models. The model of Lam and Bremhorst (1981) was developed for application to forced convective flow. Two transport equations for the kinetic energy of turbulence (k) and the dissipation rate of kinetic energy of turbulence (ε) must be solved. The turbulent viscosity calculated from k and ε is damped near the rigid surface by a wall function f_μ which is a function of two turbulent Reynolds number $Re_t = k^2/(\nu\epsilon)$ and $Re_y = k^{1/2} \cdot y/\nu$. Two wall functions ($f_1$ and f_2) are used in the transport equation of ε (see Table 3).

$$\nu_t = c_\mu \cdot f_\mu \frac{k^2}{\epsilon} \tag{8}$$

The model of Plumb and Kennedy (1977) includes a third transport equation for the mean squared temperature fluctuations $\overline{T'^2}$ to account for the contribution of buoyancy to the turbulent kinetic energy and dissipation rate. In the k-ε- and k-, ε- and $\overline{T'^2}$ -equations, wall terms were added to assign a boundary condition to $c_w = 0$ at the wall and to account for the nonisotropic behavior near the wall.

k-equation

$$\frac{\partial(\bar{u}\,k)}{\partial x} + \frac{\partial(\bar{v}\,k)}{\partial y} = \frac{\partial}{\partial y}\left[\left(\frac{\nu_t}{\sigma_k} + \nu\right)\frac{\partial k}{\partial y}\right] + \nu_t\left(\frac{\partial \bar{u}}{\partial y}\right)^2$$

$$+ g\beta c_g\left(k\overline{T'^2}\right)^{1/2} - \epsilon - 2\nu\, c_w\left(\frac{\partial(k^{1/2})}{\partial y}\right)^2 \tag{9}$$

ϵ-equation

$$\frac{\partial(\bar{u}\,\epsilon)}{\partial x} + \frac{\partial(\bar{v}\,\epsilon)}{\partial y} = \frac{\partial}{\partial y}\left[\left(\frac{\nu_t}{\sigma_\epsilon} + \nu\right)\frac{\partial \epsilon}{\partial y}\right] + c_{\epsilon 1} f_1 \frac{\epsilon}{k}\nu_t\left(\frac{\partial \bar{u}}{\partial y}\right)^2$$

$$- c_{\epsilon 2} f_2 \frac{\epsilon^2}{k} + c_{\epsilon 3} g\beta\, c_g \epsilon \left(\frac{\overline{T'^2}}{k}\right)^{1/2} \qquad (10)$$

$\overline{T'^2}$- equation

$$\frac{\partial(\bar{u}\,\overline{T'^2})}{\partial x} + \frac{\partial(\bar{v}\,\overline{T'^2})}{\partial y} = \frac{\partial}{\partial y}\left[\left(\frac{\nu_t}{\sigma_T} + \alpha\right)\frac{\partial \overline{T'^2}}{\partial y}\right] + c_{T1}\nu_t\left(\frac{\partial \bar{T}}{\partial y}\right)^2$$

$$- c_{T2}\frac{\epsilon}{k}\overline{T'^2} - 2\alpha\left(\frac{\partial(\overline{T'^2})^{1/2}}{\partial y}\right)^2 \qquad (11)$$

2.2.2 Stress models

Equations governing the transport of the Reynolds stresses and turbulent heat fluxes can be derived by manipulating the momentum and energy equations. The modeling of the unknown terms in these equations follows from the work of Launder and his colleagues (Launder, 1975; 1986; Kebede et al., 1985; Gibson and Launder, 1978; Gibson, 1978; Rodi, 1980; 1982) and is carefully outlined in Heiss (1987). The transport equations for $\overline{u'u'}$, $\overline{v'v'}$, $\overline{w'w'}$, $\overline{u'v'}$, $\overline{u'T'}$, $\overline{v'T'}$, $\overline{T'^2}$ and ϵ must be calculated because of the strong dependence of these quantities on each other. This model with 8 differential equations to determine the turbulent quantities is known as Reynolds Stress Model (RSM). The systems of the equations, the wall functions and the model constants are shown in the Appendix.

Assuming local equilibrium (convection = diffusion) in the transport equations of correlations of fluctuating quantities results in algebraic expressions. In addition to the differential equations for k and ϵ, a system of six algebraic equations must be solved (Algebraic Stress Model, ASM).

Unfortunately, the summation of the Reynolds stresses $\overline{u'u'}$, $\overline{v'v'}$ and $\overline{w'w'}$ yields only 2k for local equilibrium of the dissipation rate ϵ, the production term, $-\overline{u'v'}(\partial\bar{u}/\partial y)$, and the buoyancy induced term, $g\beta\overline{u'T'}$. To avoid this inconsistency, it is assumed the behavior of advection-diffusion in the equations of the normal Reynolds stresses is the same as in the k-equation. Then, the algebraic equations for $\overline{u'u'}$, $\overline{v'v'}$ and $\overline{w'w'}$ can be corrected (ASM_{corr}) by

$$(\text{advection} - \text{diffusion})_{\overline{u'u'}}$$

$$= (\text{advection} - \text{diffusion})_k \cdot \frac{\overline{u'u'}}{k}$$

$$= \frac{\overline{u'u'}}{k}\left(-\overline{u'v'}\frac{\partial \bar{u}}{\partial y} + g\beta\overline{u'T'} - \epsilon\right)$$

and with similar correction terms for the $\overline{v'v'}$- and $\overline{w'w'}$- equations.

The system of the algebraic equations and the correction terms are shown in the Appendix.

2.3 Numerical Scheme

A finite difference procedure was chosen for obtaining a numerical solution of the differential

Table 2: Model constants for the k-ϵ model of Lam and Bremhorst (KEM) and the k-ϵ-$\overline{T'^2}$ model of Plumb and Kennedy (KETM).

Constant	σ_k	σ_ϵ	σ_T	c_μ	c_g	c_w	$c_{\epsilon 1}$	$c_{\epsilon 2}$	$c_{\epsilon 3}$	c_{T1}	c_{T2}
KEM	1.00	1.30	-	0.09	0.00	0.00	1.44	1.92	0.00	-	-
KETM	1.00	1.30	0.90	0.09	0.50	1.00	1.44	1.92	1.44	2.80	1.70

Table 3: Turbulent Prandtl number, wall functions and boundary condition for ϵ

	k-ϵ-$\overline{T'^2}$ model (KETM)	k-ϵ model (KEM)
Pr_t	$2.5 - 2.0(y/\delta)$	0.9
f_μ	$\exp[-2.5/(1+Re_t/50)]$	$[1 - \exp(-0.0165Re_y)]^2(1 + 20.5/Re_t)$
f_1	1	$1 + (0.05/f_\mu)^3$
f_2	$1 - 0.3\exp(-Re_t^2)$	$1 - \exp(-Re_t^2)$
b. c. for ϵ	$\epsilon_w = 0$	$\left.\frac{\partial \epsilon}{\partial y}\right\|_w = 0$

equations presented in the previous section. All calculations were performed using an upwind differencing scheme in the streamwise direction, x, and power-Law scheme in the cross-stream direction, y, described by Patankar (1980). The discretization equations, implicit in the forward step, were solved using a TDMA (TriDiagonal-Matrix Algorithm). A nonuniform grid consisting of 52 nodes in the cross-stream direction, y, generated grid-independent results. The grid was expanded from the wall using a factor 1.25, and the first 5 nodes were located in the viscous sublayer ($y^+ < 4$). The forward step was 10 times the breadth of the inner control volume ($\Delta x = 10 \cdot \Delta y_1$).

2.4 Boundary Conditions

The boundary conditions for heated, vertical, flat plate flow are shown in Fig. 1.

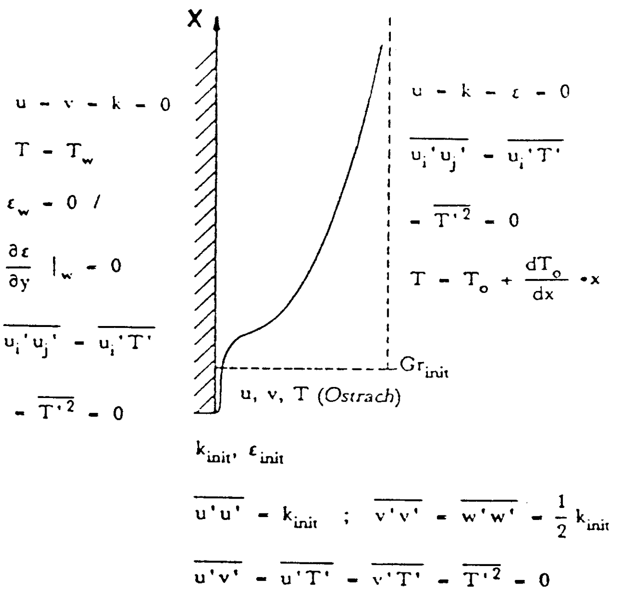

Figure 1. Boundary conditions and calculation domain.

Along the solid wall and the outer edge of the boundary layer, the streamwise velocity component and all turbulent quantities were set to zero, except ϵ at the rigid wall. According to Plumb and Kennedy this boundary condition was set equal to zero for the k-ϵ-$\overline{T'^2}$ model. For the other models the first derivation of ϵ was set equal to zero following Patel et al. (1985). Furthermore, a few calculations with $\epsilon = 2\nu\left(\frac{\partial k^{1/2}}{\partial y}\right)^2_w$ and $\epsilon_w = 2\nu\left(\frac{\partial^2 k}{\partial y^2}\right)_w$ have shown that the influence of the different boundary conditions is very small (less than 5% in the heat transfer). However, the numerical solution with $\left(\frac{\partial \epsilon}{\partial y}\right)_w = 0$ was more stable. The wall temperature T_w was constant and the environment temperature T_o was slightly increased with the height according to the experimental condition, ($dT_o/dx = 2$ K/m). Velocity and temperature distributions along the upstream boundary were specified by imposing Ostrach's (1952) laminar flow solution. To initiate turbulence according to Plumb and Kennedy at $Gr_x = 4.10^8$, a small amount of turbulent viscosity was assumed ($\nu_{t,int} = 0.01\nu$) to exist and the corresponding values of ϵ_{init} and k_{init} were calculated from an approximate balance between shearing production and rate of dissipation and from eq. (8)

$$\epsilon_{init} = \nu_{t,init}\left(\frac{\partial \bar{u}}{\partial y}\right)^2$$

$$k_{init} = \left(\nu_{t,init}\frac{\epsilon_{init}}{c_\mu}\right)^{1/2} \quad \text{with} \quad \frac{\nu_{t,init}}{\nu} = 0.01$$

For the Reynolds stress model, $\overline{u'u'} = k_{init}$ and $\overline{v'v'} = \overline{w'w'} = \frac{1}{2}k_{init}$ were imposed.

For all models the influence of the wall functions was eliminated in the outer region. Except in the region between the wall and the location of the velocity maximum the wall functions f_1, f_2 and f_μ were set equal to 1 and f_s and f_ℓ were set equal to 0.

3. RESULTS

The results predicted by the three mixing-length models (MMA, MMB, MMC), k-ϵ model (KEM), k-ϵ-$\overline{T'^2}$ model (KETM) and the three stress models (RSM, ASM, ASM_{corr}) are presented in the following subsections. The results are compared with the experimental data reported by Cheesewright and Ierokipiotis (1982) and Miyamoto et al. (1982).

Figure 2a shows the nondimensional streamwise velocity profile [$u_b = 2(g\beta\Delta Tx)^{1/2}$] for the three mixing-length models of $Gr_x = 5.67 \times 10^{10}$ as a function of the nondimensional traverse coordinate, $\zeta = \frac{y}{x} Nu_x$. All three models predict the location of the velocity maximum well, however, model MMB and MMC show an overshoot of the velocity maximum, and an undershoot of the velocity in the outer region because the two models yields too small turbulent viscosity.

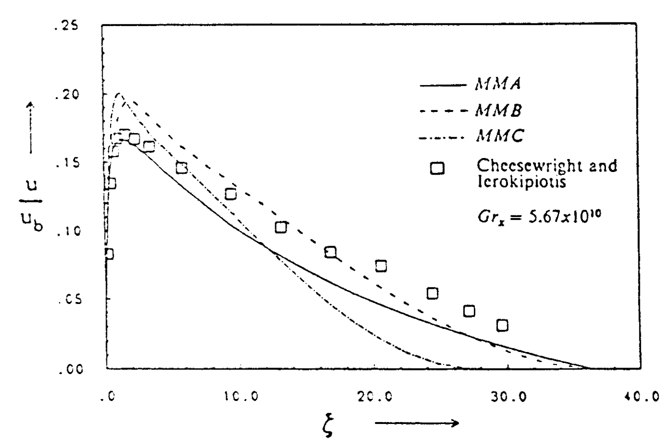

Figure 2a: Streamwise velocity profiles calculated by mixing-length models version A, B, and C.

Figure 2b shows the velocity profiles calculated by the KEM and KETM models. The KEM prediction is consistently good for all values of the transverse coordinate. As a result of a higher turbulent energy, the velocity predicted by KETM is too small everywhere.

Figure 2c shows the velocity profiles for the three stress models. All the predictions of velocity are in reasonable agreement with LDV measurements, however, the velocity maximum, calculated by RSM, is located too far from the wall, and the velocity, predicted by ASM, falls below the experimental data in the outer region.

The reason is the $\overline{u'v'}$ distribution. Although $\overline{u'v'}$ calculated by RSM agrees much better with experimental data (Fig. 4e) in the region $\zeta < 6$ than these calculated by ASM or ASM_{corr}, the slope of the velocity profile is too small in the near wall region.

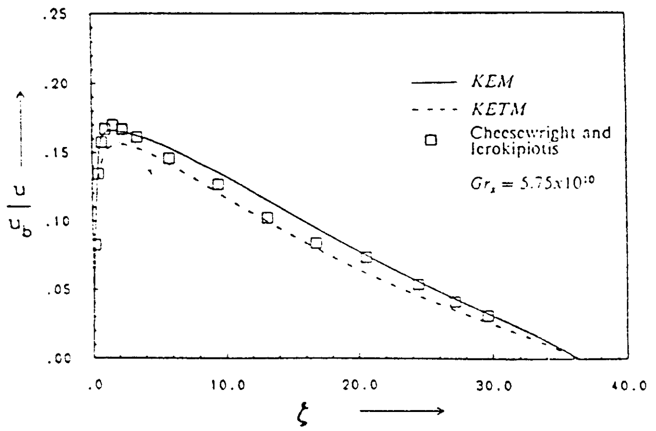

Figure 2b: Streamwise velocity profiles calculated by k-ϵ model (KEM) and k-ϵ-T'^2 model (KETM).

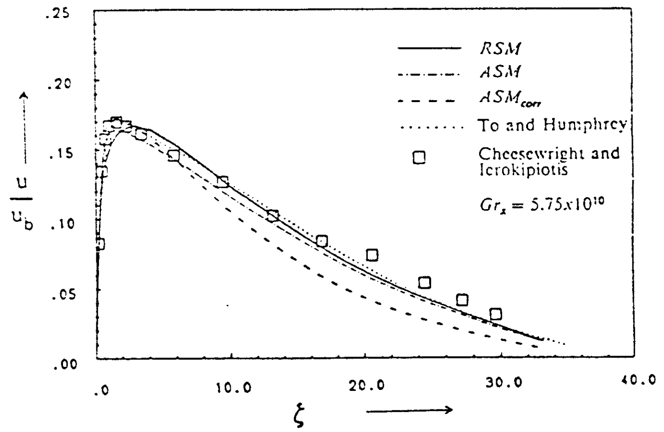

Figure 2c: Streamwise velocity profiles calculated by Reynolds stress model, algebraic stress model and corrected alebraic stress model.

The numerical calculations of the Nusselt number dependence on Grashof number shown in Figures 3a-3c agree with the experimental data very well in the fully developed turbulent region with the exception of MMB and MMC. The transition from laminar to turbulent flow is indicated by the change in heat transfer. Because of the inadequacies of the lacking transport equations for turbulent quantities, the mixing-length models are not able to predict a smooth transition. Although the other models initialize the turbulence at $Gr_x = 4 \times 10^8$, the transition occurs at $Gr_x > 10^9$.

Figures 4a-4f show the mean temperature profiles, the mean squared temperature fluctuation, the Reynolds stresses and the turbulent heat fluxes calculated by the stress models at $Gr^*_x = Gr_x \cdot Nu_x = 6.68 \cdot 10^{13}$ and compare the experimental results reported by Miyamoto et al. (1982) and the numerical results from To and Humphrey (1986). They used an uncorrected algebraic stress model similar to the ASM in this study. All profiles show good agreement with the experimental data except the $\overline{v'T'}$ distribution. But using the low measured $\overline{v'T'}$ values in the energy-equation yields very poor Nusselt numbers. The reason for this discrepancy could be the very low horizontal velocity v (lower than 1 mm/s), the 'beam dancing' in the y direction caused by inhomogeneous refractive index, and the distance between the thermocouple and the measuring volume of the LDV, which was 2 mm in streamwise direction according to Miyamoto et al. (1982). Therefore, it is very hard to measure T'^2.

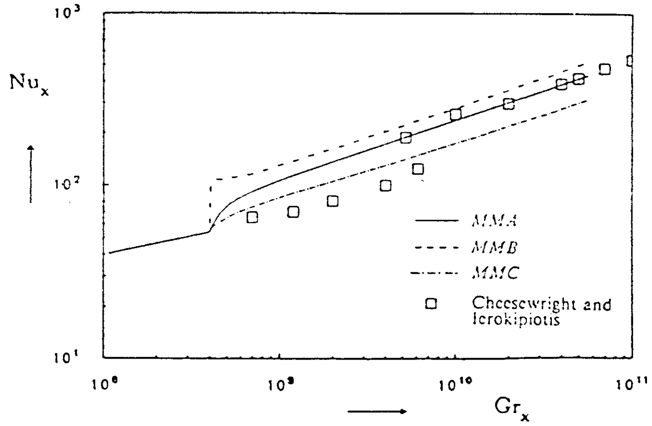

Figure 3a: Heat transfer along the plate calculated by mixing-length models.

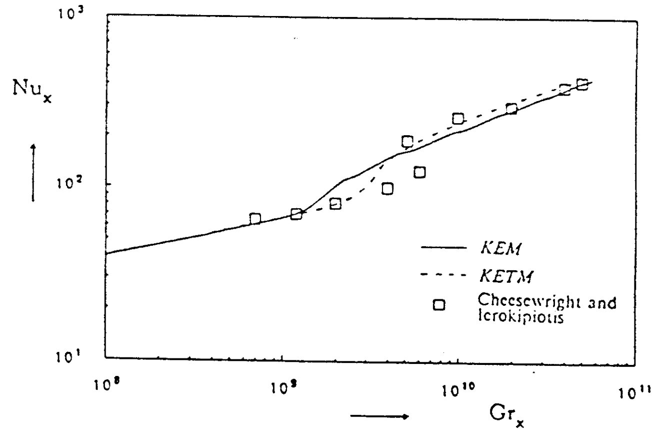

Figure 3b: Heat transfer along the plate calculated by k-ϵ and k-ϵ-T'^2 model.

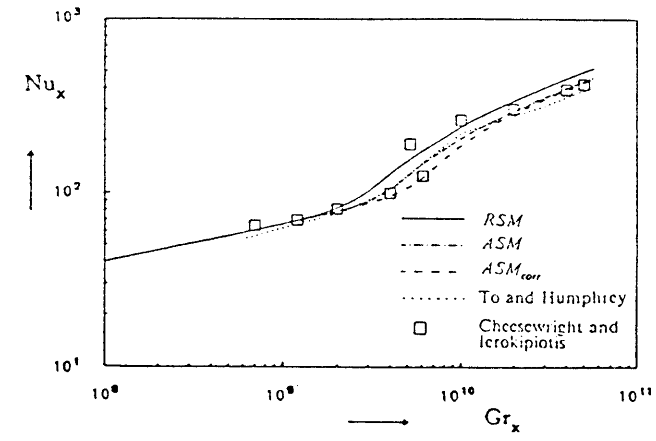

Figure 3c: Heat transfer along the plate calculated by the stress models.

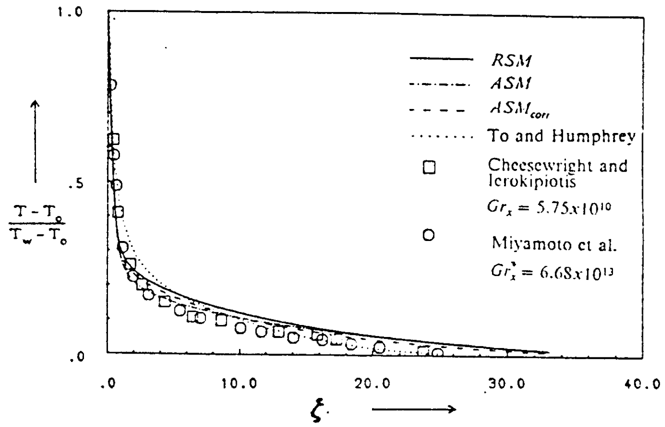

Figure 4a: Mean temperature distribution calculated by stress models.

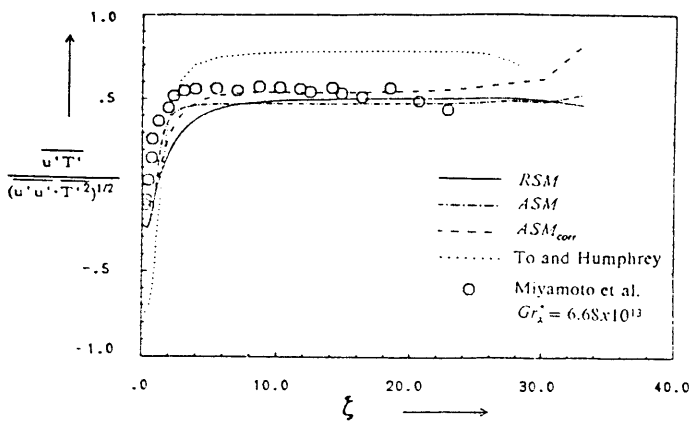

Figure 4d: Turbulent heat flux $\overline{u'T'}$ calculated by stress models.

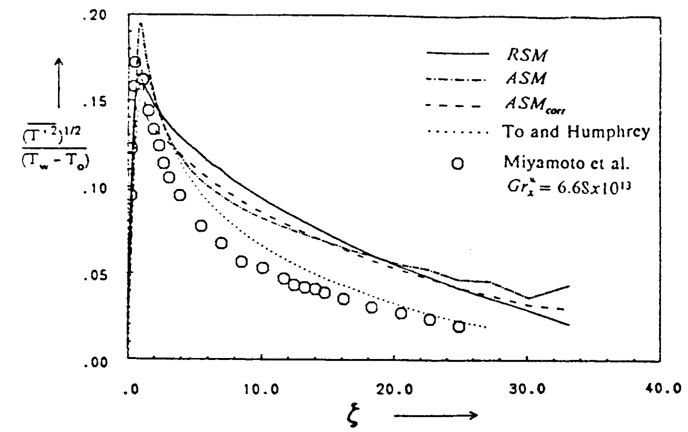

Figure 4b: Mean squared temperature fluctuations calculated by stress models.

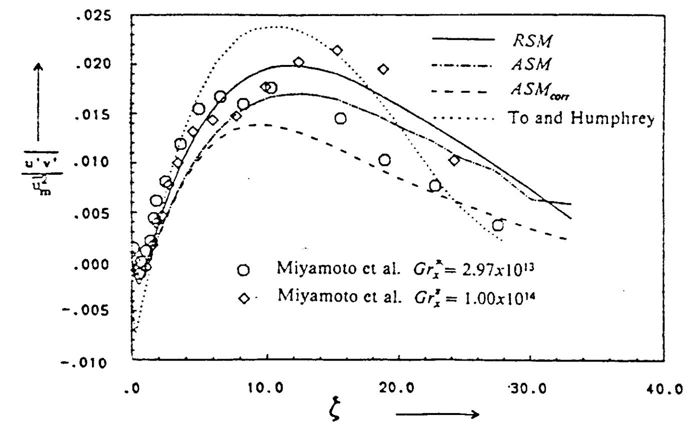

Figure 4e: Turbulent shear stress calculated by stress models.

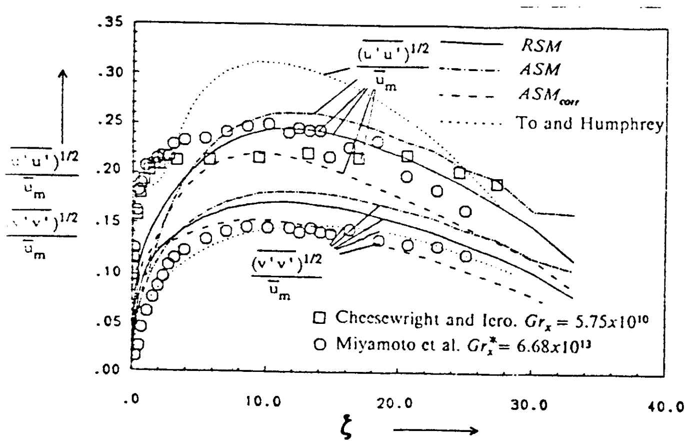

Figure 4c: Normal Reynolds stresses calculated by stress models.

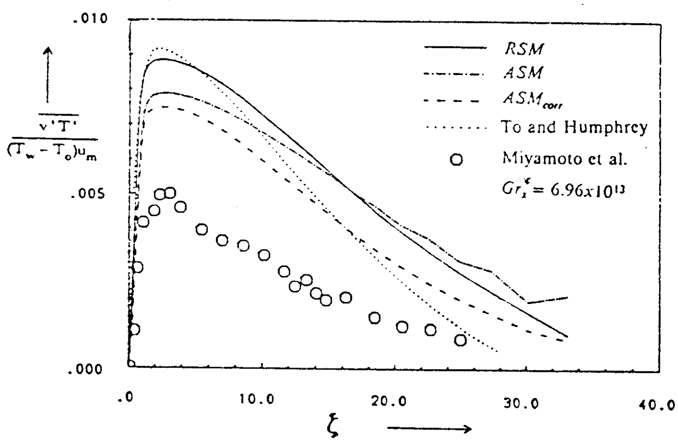

Figure 4f: Turbulent heat flux $\overline{v'T'}$ calculated by stress models.

4. DISCUSSION

As shown above, all the models yield reasonable results. Unfortunately, the mixing-length models where one does not solve differential equations for the turbulent quantities, are not able to predict the transition from laminar to turbulent flow. Further, the other models need to introduce a small amount of turbulent viscosity at some point create a numerical transition. Figure 5 shows the influence of introducing turbulence at different points. All these models need the knowledge from experiments to locate where the transition should occur. However, the transition region in the experiments are also dependent on existing disturbances.

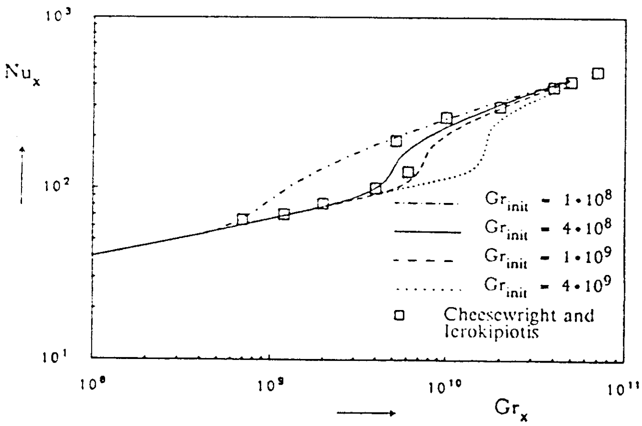

Figure 5: Influence of introducing turbulence at different points calculated by KETM.

The mixing-length model, the k-ε model and the k-ε-T' model use the gradient assumption for $\overline{u'v'}$. According to Cheesewright and Dastbaz (1983), there is a region between the wall and the velocity maximum where $\overline{u'v'}$ and the velocity gradient are both positive ($y_1 < y < y_2$ in Fig. 6). Thus, equation (4) is only satisfied for negative turbulent viscosity which is numerically and physically unrealistic. As a result, the stress models predict the production of $\overline{u'v'}$ due to buoyancy correctly.

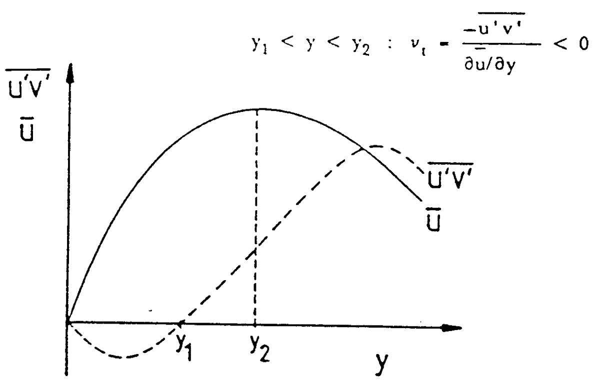

Figure 6: Mean velocity and $\overline{u'v'}$ profile according to Cheesewright and Dastbaz (1983).

The turbulent Prandtl number, Pr_t, which does not arise in the stress models, is a critical parameter in the mixing-length models, k-ε model and k-ε-T'^2 model. Plumb and Kennedy chose the distribution of Pr_t, to yield the best agreement with experiments. Although, Pr_t has a significant effect on the heat transfer, natural convection experimental data are completely lacking in the literature.

Using the Reynolds averaged boundary-layer equations the mean velocity depends only on the gradient of $\overline{u'v'}$ (besides $\bar{v}$ and $\bar{T}$) and the heat transfer depends only on the gradient of $\overline{v'T'}$. Calculations were performed, so that the two quantities, $\overline{u'v'}$ and $\overline{v'T'}$, were tuned to agree with the experiment data by adjusting several constants. However, the results (mean velocity and heat transfer) were very poor. There is a need for more experimental data to improve the turbulence models, especially in the near wall region.

This study shows that the model of Lam and Bremhorst (1981) is the best tool for calculation of turbulent vertical convective flow considering the quality of the results and the computer cost, if the Reynolds stresses and the turbulent heat flux are not of interest.

ACKNOWLEDGEMENT

Part of this research was performed while the first author was at the Department of Mechanical, Aerospace and Nuclear Engineering, Univesity of California, Los Angeles, as a recipient of a scholarship from "Wissenschaftsausschuss der NATO provided by DAAD". The support is gratefully acknowledged.

REFERENCES

Cebeci, T. and Khattab, A., 1975, "Prediction of Turbulent-Free-Convective-Heat Transfer from a Vertical Flat Plate", Journal of Heat Transfer, 97, pp. 469-471.

Cheesewright, R. and Dastbaz, A., 1983, "The Structure of Turbulence in a Natural Convection Boundary Layer; Proc. 4th Turbulent Shear Flow Symposium, pp. 17.25-17.29, Karlsruhe.

Cheesewright, R. and Ierokiopitis, E., 1982, "Velocity Measurements in a Turbulent Natural Convection Boundary Layer", Proc. 7th Int. Heat Transfer Conference, 2, pp. 305-309, München.

Escudier, M. 1966, "The Distribution of Mixing-Length in Turbulent Flow Near Walls, Heat Transfer Section Report TWF/1, Imperial College, London.

Gibson, M.M. and Launder, B.E., 1978 "Ground Effects on Pressure Fluctuations in the Atmospheric Boundary Layer", Journal of Fluid Mechanics, 86, pp. 491-511.

Gibson, M.M., 1978, "An Algebraic Stress and Heat-Flux Model for Turbulent Shear Flow with Streamline Curvature", Int. J. Heat and Mass Transfer, 21, pp. 1609-1617.

Heiss, A., 1987, "Numerische und experimentelle Untersuchungen der laminaren und turbulenten Konvektion in einem geschlossenen Behaelter", Dissertation am Lehrstuhl A fuer Thermodynamik, Technische Universitaet Muenchen.

Humphrey, J. and To, W., 1985, "Numerical Prediction of Turbulent Free Convection along a Heated Vertical Flat Plate", Proc. 5th Turbulent Shear Flow Symposium, pp. 22.19-22.25, Cornell.

Kebede, W., Launder, B.E. and Younis, B., 1985, "Large Amplitude Periodic Pipe Flow: A Second-Moment Closure Study", Proc. 5th Turbulent Shear Flow Symposium, pp. 16.23-16.29, Cornell.

Lam, C. and Bremhorst, B., 1981, "A Modified Form of the k-ε-Model for Predicting Wall Turbulence", Journal of Fluids Engineering, 103, pp. 456-460.

Launder, B.E., 1975, "On the Effects of a Gravitational Field on the Turbulent Transport of Heat and Momentum", Journal of Fluid Mechanics, 67, pp. 569-581.

Launder, B.E., 1986, "Low-Reynolds-Number Turbulence near Walls", Department of Mechanical Engineering, University of Manchester, Report TFD/86/4.

Miyamato, M., Kajino, H., Kurmia, J., and Takanami, I., 1982, "Development of Turbulence Characteristics in a Vertical Free Convection Boundary Layer", Proc. 7th Int. Heat Transfer Conference, 2, pp. 323-328, München.

Noto, K. and Matsumoto R., 1975, "Turbulent Heat Transfer by Natural Convection Along an Isothermal Vertical Flat Surface", Journal of Heat Transfer, 97, pp. 621-624.

Ostrach, S., 1952, "An Analysis of Laminar Free-Convection Flow and Heat Transfer about a Flat Plate Parallel to the Direction of the Generating Body Force", NACA TN 2635, Report 1111.

Patankar, S.V., 1980, Numerical Heat Transfer and Fluid Flows, Hemisphere Publishing Corporation, McGraw-Hill Book Company.

Patel, V., Rodi, W., Scheurer, G., 1985, "A Review and Evaluation of Trublence Models for Near Wall and Low-Reynolds-Numer Flows," AIAA Journal, 23, No. 9.

Plumb, O., and Kennedy, L.A., 1977, "Application of a k-ε-Turbulence Model to Natural Convection from a Vertical Isothermal Surface", Journal of Heat Transfer, 99, pp. 79-85.

Rodi, W., 1980, "Turbulence Models and their Application in Hydraulics", State-of-the-Art Paper, Karlsruhe.

Rodi, W., 1982, "Turbulent Buoyant Jets and Plumes", Pergamon Press.

To, W. and Humphrey, J., 1986, "Numerical Simulation of Buoyant Turbulent Flow-Free Convection Along a Heated Vertical, Flate Plate," Int. J. Heat Mass Transfer, 29, pp. 573-592.

APPENDIX

Reynolds Stress Model (RSM)

$\overline{u'u'}$-equation

$$\frac{\partial(\bar{u}\,\overline{u'u'})}{\partial x} + \frac{\partial(\bar{v}\,\overline{u'u'})}{\partial y} =$$

$$\frac{\partial}{\partial y}\left[\left(c_s \frac{k}{\epsilon}\overline{v'v'} + \nu\right)\frac{\partial \overline{u'u'}}{\partial y}\right] - 2\overline{u'v'}\frac{\partial \bar{u}}{\partial y} +$$

$$2g\beta\overline{u'T'} - \frac{2}{3}\epsilon\left[(1 - f_s) + \frac{3}{2} f_s \frac{\overline{u'u'}}{k}\right] -$$

$$c_1 \frac{\epsilon}{k}\left(\overline{u'u'} - \frac{2}{3}k\right) + \frac{4}{3} c_2 \overline{u'v'}\frac{\partial \bar{u}}{\partial y} - \frac{4}{3} c_3 g\beta\overline{u'T'} -$$

$$c_{1S} f_\ell \frac{\epsilon}{k}\overline{v'v'} - \frac{2}{3} c_{2S} c_2 f_\ell \overline{u'v'}\frac{\partial \bar{u}}{\partial y} + \frac{2}{3} c_{3S} c_3 f_\ell g\beta\overline{u'T'} \quad (A.1)$$

$\overline{v'v'}$-equation

$$\frac{\partial(\bar{u}\,\overline{v'v'})}{\partial x} + \frac{\partial(\bar{v}\,\overline{v'v'})}{\partial y} = \frac{\partial}{\partial y}\left[\left(c_s \frac{k}{\epsilon}\overline{v'v'} + \nu\right)\frac{\partial \overline{v'v'}}{\partial y}\right]$$

$$- \frac{2}{3}\epsilon\left[(1 - f_s) + \frac{3}{2} f_s \frac{\overline{v'v'}}{k}\right] - c_1 \frac{\epsilon}{k}\left(\overline{v'v'} - \frac{2}{3}k\right)$$

$$- \frac{2}{3} c_2 \overline{u'v'}\frac{\partial \bar{u}}{\partial y} + \frac{2}{3} c_3 g\beta\overline{u'T'} - 2c_{1S} f_\ell \frac{\epsilon}{k}\overline{v'v'}$$

$$+ \frac{4}{3} c_{2S} c_2 f_\ell \overline{u'v'}\frac{\partial \bar{u}}{\partial y} - \frac{4}{3} c_{3S} c_3 f_\ell g\beta\,\overline{u'T'} \quad (A.2)$$

$\overline{w'w'}$-equation

$$\frac{\partial(\bar{u}\,\overline{w'w'})}{\partial x} + \frac{\partial(\bar{v}\,\overline{w'w'})}{\partial y} = \frac{\partial}{\partial y}\left[\left(c_s \frac{k}{\epsilon}\overline{v'v'} + \nu\right)\frac{\partial \overline{w'w'}}{\partial y}\right]$$

$$- \frac{2}{3}\epsilon\left[(1 - f_s) + \frac{3}{2} f_s \frac{\overline{w'w'}}{k}\right] - c_1 \frac{\epsilon}{k}\left(\overline{w'w'} - \frac{2}{3}k\right)$$

$$- \frac{2}{3} c_2 \overline{u'v'}\frac{\partial \bar{u}}{\partial y} + \frac{2}{3} c_3 g\beta\overline{u'T'} + c_{1S} f_\ell \frac{\epsilon}{k}\overline{v'v'}$$

$$- \frac{2}{3} c_{2S} c_2 f_\ell \overline{u'v'}\frac{\partial \bar{u}}{\partial y} + \frac{2}{3} c_{3S} c_3 f_\ell g\beta\,\overline{u'T'} \quad (A.3)$$

with $k = \frac{1}{2}\left(\overline{u'u'} + \overline{v'v'} + \overline{w'w'}\right)$

$\overline{u'v'}$-equation

$$\frac{\partial(\bar{u}\,\overline{u'v'})}{\partial x} + \frac{\partial(\bar{v}\,\overline{u'v'})}{\partial y} = \frac{\partial}{\partial y}\left[\left(c_s \frac{k}{\epsilon}\overline{v'v'} + \nu\right)\frac{\partial \overline{u'v'}}{\partial y}\right]$$

$$- \overline{v'v'}\frac{\partial \bar{u}}{\partial y} + g\beta\,\overline{v'T'} - \epsilon f_s \frac{\overline{u'v'}}{k} - c_1\frac{\epsilon}{k}\overline{u'v'}$$

$$+ c_2\,\overline{v'v'}\frac{\partial \bar{u}}{\partial y} - c_3 g\beta\,\overline{v'T'} - \frac{3}{2}c_{1S}f_\ell\frac{\epsilon}{K}\overline{u'v'}$$

$$- \frac{3}{2}c_{2S}c_2 f_\ell\,\overline{v'v'}\frac{\partial \bar{u}}{\partial y} + \frac{3}{2}c_{3S}c_3 f_\ell g\beta\,\overline{v'T'} \qquad (A.4)$$

$\overline{u'T'}$-equation

$$\frac{\partial(\bar{u}\,\overline{u'T'})}{\partial x} + \frac{\partial(\bar{v}\,\overline{u'T'})}{\partial y}$$

$$= \frac{\partial}{\partial y}\left[c_T\frac{k}{\epsilon}\left(\overline{u'v'}\frac{\partial\overline{v'T'}}{\partial y} + \overline{v'v'}\frac{\partial\overline{u'T'}}{\partial y}\right) + \frac{\alpha+\nu}{2}\frac{\partial\overline{u'T'}}{\partial y}\right]$$

$$- \left[\overline{u'v'}\frac{\partial \bar{T}}{\partial y} + \overline{v'T'}\frac{\partial \bar{u}}{\partial y}\right] + g\beta\overline{T'^2} - c_{4uT}\epsilon f_s\frac{\overline{u'T'}}{k}$$

$$- c_{1T}\frac{\epsilon}{k}\overline{u'T'} + c_{2T}\overline{v'T'}\frac{\partial \bar{u}}{\partial y} - c_{3T}g\beta\overline{T'^2} \qquad (A.5)$$

$\overline{v'T'}$-equation

$$\frac{\partial(\bar{u}\,\overline{v'T'})}{\partial x} + \frac{\partial(\bar{v}\,\overline{v'T'})}{\partial y} = \frac{\partial}{\partial y}\left[\left(2c_T\frac{k}{\epsilon}\overline{v'v'} + \frac{\alpha+\nu}{2}\right)\frac{\partial\overline{v'T'}}{\partial y}\right]$$

$$- \overline{v'v'}\frac{\partial \bar{T}}{\partial y} - c_{4vT}\epsilon f_s\frac{\overline{v'T'}}{k} - c_{1T}\frac{\epsilon}{k}\overline{v'T'} - c_{1TS}f_\ell\frac{\epsilon}{k}\overline{v'T'} \qquad (A.6)$$

$\overline{T'^2}$-equation

$$\frac{\partial(\bar{u}\,\overline{T'^2})}{\partial x} + \frac{\partial(\bar{v}\,\overline{T'^2})}{\partial y} = \frac{\partial}{\partial y}\left[\left(c_{TT}\frac{k}{\epsilon}\overline{v'v'} + \alpha\right)\frac{\partial\overline{T'^2}}{\partial y}\right]$$

$$- 2\overline{v'T'}\frac{\partial \bar{T}}{\partial y} - \frac{1}{R}\frac{\overline{T'^2}}{k}\epsilon \qquad (A.7)$$

ϵ-equation (the same for ASM and ASM_{corr})

$$\frac{\partial(\bar{u}\,\epsilon)}{\partial x} + \frac{\partial(\bar{v}\,\epsilon)}{\partial y} = \frac{\partial}{\partial y}\left[\left(c_\epsilon\frac{k}{\epsilon}\overline{v'v'} + \nu\right)\frac{\partial \epsilon}{\partial y}\right]$$

$$+ c_{\epsilon 1}f_1\frac{\epsilon}{k}\left(-\overline{u'v'}\frac{\partial \bar{u}}{dy} + g\beta\overline{u'T'}\right) - c_{\epsilon 2}f_2\frac{\epsilon^2}{k}$$

$$+ c_{\epsilon 3}\,\nu\frac{k}{\epsilon}\overline{v'v'}\left(\frac{\partial^2\bar{u}}{\partial y^2}\right)^2 + c_{\epsilon 4}f_s f_\ell\frac{\epsilon}{k}\left(-\overline{u'v'}\frac{\partial \bar{u}}{\partial y}\right) \qquad (A.8)$$

Algebraic Stress Model (ASM)

$$\overline{u'u'} = \frac{2k}{3\epsilon(c_1 + f_s)}\Big[-(3 - 2c_2 + c_2c_{2S}f_\ell)\overline{u'v'}\frac{\partial \bar{u}}{\partial y}$$

$$+ (3 - 2c_3 + c_3c_{3S}f_\ell)g\beta\,\overline{u'T'}$$

$$+ (c_1 - 1 + f_s)\epsilon + c_{1S}f_\ell\frac{\epsilon}{k}\overline{v'v'}\Big] \qquad (A.9)$$

$$\overline{v'v'} = \frac{2k}{3\epsilon(c_1 + f_s + 2c_{1S}f_\ell)}\Big[-c_2(1 - 2c_{2S}f_\ell)\,\overline{u'v'}\frac{\partial \bar{u}}{\partial y}$$

$$+ c_3(1 - 2c_{3S}f_\ell)g\beta\overline{u'T'} + (c_1 - 1 + f_s)\epsilon\Big] \qquad (A.10)$$

$$\overline{w'w'} = \frac{2k}{3\epsilon(c_1 + f_s)}\Big[-c_2(1 - 2c_{2S}f_\ell)\,\overline{u'v'}\frac{\partial \bar{u}}{\partial y}$$

$$+ c_3(1 - 2c_{3S}f_1)g\beta\overline{u'T'} + (c_1 - 1 + f_s)\epsilon$$

$$+ c_{1S}f_\ell\frac{\epsilon}{K}\overline{v'v'}\Big] \qquad (A.11)$$

[$\overline{w'w'}$ - equation not necessary for solving the system]

$$\overline{u'v'} = \frac{k}{\epsilon(c_1 + f_s + 1.5c_{1S}f_\ell)}\Big[(-c_2 - 1$$

$$- \frac{3}{2}c_2c_{2S}f_\ell)\,\overline{v'v'}\frac{\partial \bar{u}}{\partial y} - (c_3 - 1 - \frac{3}{2}c_3c_{3S}f_\ell)g\beta\overline{v'T'}\Big] \qquad (A.12)$$

$$\overline{u'T'} = \frac{k}{\epsilon(c_{1T} + c_{4uT}f_s)}\Big[-\overline{u'v'}\frac{\partial \bar{T}}{\partial y} - (1 - c_{2T})\,\overline{v'T'}\frac{\partial \bar{u}}{\partial y}$$

$$+ (1 - c_{3T})g\beta\overline{T'^2}\Big] \qquad (A.13)$$

$$\overline{v'T'} = \frac{k}{\epsilon(c_{1T} + c_{1TS}f_\ell + c_{4vT}f_s)}\left[-\overline{v'v'}\frac{\partial \bar{T}}{\partial y}\right] \qquad (A.14)$$

$$\overline{T'^2} = \frac{k}{\epsilon}\left[-2R\overline{v'T'}\frac{\partial \bar{T}'}{\partial y}\right] \qquad (A.15)$$

"corrected" Algebraic Stress Model (ASM_{corr}) additional terms for (A.8-A.10)

$$\overline{u'u'}\text{ - eq.:}\quad \frac{2\,\overline{u'u'}}{3\epsilon(c_1 + f_s)}\left[\overline{u'v'}\frac{\partial \bar{u}}{\partial y} - g\beta\overline{u'T'} + \epsilon\right] \qquad (A.16)$$

$\overline{v'v'}$ - eq.: $\frac{2\ \overline{v'v'}}{3\epsilon(c_1 + c_{1S}f_\ell + f_s)}\ [\overline{u'v'}\ \frac{\partial \bar{u}}{\partial y} - g\beta\overline{u'T'} + \epsilon]$

(A.17)

$\overline{w'w'}$ - eq.: $\frac{2\ \overline{w'w'}}{3\epsilon(c_1 + f_s)}\ [\overline{u'v'}\ \frac{\partial \bar{u}}{\partial y} - g\beta\overline{u'T'} + \epsilon]$

(A.18)

k - equation

$$\frac{\partial(\bar{u}\ \bar{k})}{\partial x} + \frac{\partial(\bar{u}\ \bar{k})}{\partial y} = \frac{\partial}{\partial y}\left[\left(c_s \frac{k}{\epsilon} + \nu\right) \frac{\partial k}{\partial y}\right]$$

$$- \overline{u'v'}\ \frac{\partial \bar{u}}{\partial y} + g\beta\overline{u'T'} - \epsilon \qquad \text{(A.19)}$$

Model-Constants for RSA, ASN and ASN_{corr}

constant	c	c_T	c_{TT}	c_ϵ	c_1	c_{1S}	c_2	c_{2S}
value	0.24	0.11	0.13	0.15	2.20	0.60	0.55	0.30

constant	c_3	c_{3S}	c_{1T}	c_{1TS}	c_{2T}	c_{2TS}	c_{3T}	c_{3TS}
value	0.55	0.00	3.00	0.50	0.50	0.00	0.50	1.00

constant	c_{4uT}	c_{4vT}	$c_{\epsilon 1}$	$c_{\epsilon 2}$	$c_{\epsilon 3}$	$c_{\epsilon 4}$	R
value	1.20	1.20	1.44	1.92	0.30	2.00	0.8

Wall functions:

$f_1 = 1$; $\qquad f_2 = 1 - 0.3\exp(-Re_t^2)$

$f_s = \exp(-Re_t/40)$; $\qquad f_\ell = \frac{(\overline{u'v'})^{3/4}}{0.41 \cdot \epsilon \cdot y}$;

with $Re = \frac{k_2}{\nu \cdot \epsilon}$